The Effect of β-Turn Structure on the Permeation of Peptides Across Monolayers of Bovine Brain Microvessel Endothelial Cells

Mette Sorensen,[1] Betina Steenberg,[1] Gregory T. Knipp,[2] Wen Wang,[2] Bente Steffansen,[1] Sven Frokjaer,[1] and Ronald T. Borchardt[2,3]

Received April 4, 1997; accepted July 17, 1997

Purpose. To investigate the effects of the β-turn structure of a peptide on its permeation via the paracellular and transcellular routes across cultured bovine brain microvessel endothelial cell (BBMEC) monolayers, an *in vitro* model of the blood-brain barrier (BBB).

Methods. The effective permeability coefficients (P_{eff}) of the model peptides were determined across BBMEC monolayers. The dimensions of the aqueous pores in the tight junctions (TJs) of the BBMEC monolayers were determined using a series of hydrophilic permeants. This value and the molecular radius of each peptide were used to calculate the theoretical paracellular ($P_\ddagger^*$) and transcellular ($P_\dagger^*$) permeability coefficients for each peptide.

Results. A comparison of the theoretical $P_\ddagger^*$ values with the observed P_{eff} values was made for a series of model peptides. For the most hydrophobic peptides (Ac-PheProXaaIle-NH_2 and Ac-PheProXaaIle-Val-NH_2; Xaa = Gly, Ile), it was concluded that the Gly-containing peptide of each pair more readily permeates BBMEC monolayers via the transcellular pathway than the Ile-containing analog. In addition, the Gly-containing peptides, which exhibit more β-turn structure, were shown to be more lipophilic than the Ile-containing peptides as estimated by the log of their 1-octanol:HBSS partition coefficients (log $P_{o/w}$). However, the three hydrophilic peptide pairs (Ac-TyrProXaaAsp-Val-NH_2, Ac-TyrProXaaAsnVal-NH_2, and Ac-TyrProXaaIleVal-NH_2; Xaa = Gly, Ile) were found to permeate BBMEC monolayers predominantly via the paracellular pathway. No differences were observed in the P_{eff} values of the hydrophilic peptides having higher β-turn structures as compared to the peptides lacking these structural features. In addition, the Ile-containing peptides exhibited significantly higher log $P_{o/w}$ values than the Gly-containing hydrophilic peptides.

Conclusions. Hydrophobic peptides that exhibit significant β-turn structure in solution are more lipophilic as measured by log $P_{o/w}$, and more readily permeate BBMEC monolayers via the transcellular route than hydrophobic peptides that lack this type of solution structure. Similar secondary structural features in hydrophilic peptides do not appear to sufficiently alter the physicochemical properties of the peptides so as to alter their paracellular flux through BBMEC monolayers.

KEY WORDS: peptide delivery; transcellular diffusion; solution conformation; BBMEC monolayers; bovine brain microvessel endothelial cells, passive diffusion.

INTRODUCTION

The clinical development of peptides and peptidomimetics for the treatment of neurological disorders has been restricted because of their limited permeation across the blood-brain barrier (BBB) (1–3). The BBB consists of brain microvessel endothelial cells (BMECs), which constitute the capillaries that perfuse the brain (4–7). The BMECs are characterized by their tight junctional (TJ) complexes, which act as a physical barrier, restricting paracellular flux of drugs and thus limiting permeation of most central nervous system active drugs to the transcellular route (1,8). The BMECs are also very metabolically active (1,9) and exhibit polarized efflux systems (10), which may further restrict permeation of drugs into the brain.

Successful clinical development of neuroactive peptides will depend, therefore, on the utilization of drug design strategies that will improve their BBB permeation without changing their biological activity (3,11). It is generally accepted that size, hydrophobicity and hydrogen bonding potential are crucial physicochemical properties in determining the ability of a peptide to permeate the BBB via the transcellular route (3,12–14). Peptide permeation of other cell monolayers has also been shown to be dependent on charge (15). Less well recognized, however, is the fact that the secondary structure (i.e. β-turn) of a peptide may affect one or more of these physicochemical properties, thus influencing its BBB permeability. Recently, our laboratory has shown that secondary structures induced by cyclizing peptides can dramatically influence their permeation through Caco-2 cell monolayers, a model of the intestinal mucosa (16–18). Similarly, we have recently shown that linear peptides that have a high propensity to form β-turn structures in solution are better able to permeate across Caco-2 cell monolayers than peptides that do not exhibit this type of secondary structure (19).

In the present study, we have designed experiments to investigate whether β-turn structures in solution can influence the permeability of a linear peptide across the BBB. For these studies, we have used five pairs of model penta- and tetrapeptides. Within each pair, the Gly-containing peptides (e.g., Ac-TyrProGlyAspVal-NH_2) have been shown to have a higher propensity to form β-turn structures in solution than do the Ile-containing peptides (e.g., Ac-TyrProIleAspVal-NH_2) (19). In addition, we have used peptides that range from hydrophilic (e.g., Ac-TyrProXaaAspVal-NH_2; Xaa = Gly, Ile) to hydrophobic (e.g., Ac-PheProXaaIle-NH_2; Xaa = Gly, Ile) so that we could determine how secondary structure affects permeation via both the paracellular (hydrophilic route) and transcellular (lipophilic route) pathways.

For these studies, we have utilized an *in vitro* cell culture model of the BBB which consists of bovine BMECs (BBMECs) grown on microporous filter supports (20,21). Since we are particularly interested in differentiating the effects of β-turn

[1] Department of Pharmaceutics, The Royal Danish School of Pharmacy, Copenhagen, Denmark.

[2] Department of Pharmaceutical Chemistry, 2095 Constant Ave., The University of Kansas, Lawrence, Kansas 66047.

[3] To whom correspondence should be addressed. (e-mail: Borchardt@smissman.hbc.ukans.edu)

ABBREVIATIONS: BBB, blood-brain barrier; BMECs, brain microvessel endothelial cells; BBMECs, bovine brain microvessel endothelial cells; TJs, tight junctions; $P_{o/w}$, partition coefficient between 1-octanol and HBSS; P_{eff}, effective permeability coefficient; $P_{ABL/F/C}$, permeability coefficient across a collagen coated Transwell® in the absence of cells; P_P, calculated paracellular permeability coefficient; P_M^*, calculated permeability coefficient across the cell monolayer; $P_\dagger^*$, transcellular permeability coefficient; $P_\ddagger^*$, theoretical paracellular permeability coefficient; ACN, acetonitrile; TFA, trifluoroacetic acid; AP, apical; BL, basolateral; HBSS, Hanks' balanced salt solution; HEPES, N-2-hydroxyethylpiperazine-N′-2-ethanesulfonate; PC, palmitoyl-DL-carnitine.

0724-8741/97/1000-1341$12.50/0

structure on the permeation of the peptides by both the paracellular and transcellular routes, it was necessary to characterize the paracellular route of transport across the BBMEC monolayers using the Renkin molecular sieving function (22,23) and paracellular permeants which varied in size and charge in order to estimate the radius of the aqueous pores through the BBMEC TJs. Knowing the radius of the aqueous pores in the TJs, it was then possible to estimate the permeability coefficients for the peptides through both the paracellular and transcellular pathways.

MATERIALS AND METHODS

Materials

Sucrose, urea, formic acid, lactic acid, and methylamine were purchased as [^{14}C]-labeled stock solutions from the American Radiolabeled Company (St. Louis, MO). Rhodamine phalloidin, platelet-poor horse serum, fibronectin, gentamicin sulfate, heparin, Percoll, N-2-hydroxyethylpiperazine-N'-2-ethanesulfonate (HEPES) and atenolol were purchased from Sigma Chemical Company (St. Louis, MO). Hanks' balanced salt solution (HBSS) was purchased from JRH Biosciences (Lenexa, KS). Collagenase/dispase and dispase were purchased from Boehringer-Mannheim (Mannheim, Germany). Ham's F-12 medium and minimum essential medium were purchased from Mediatech (Washington, D.C.). Transwells® with cell culture-treated polycarbonate membranes were purchased from Corning Costar Corporation (Cambridge, MA). 3a70B Complete counting scintillation cocktail was purchased from Research Products International (Mount Prospect, IL). Type I rat tail collagen and endothelial cell growth supplement were purchased from Collaborative Research (Lexington, MA). The N- and C-terminally capped peptides were synthesized using solid-phase methodology on a 4-(2',4'-dimethoxyphenyl-FMOC-aminomethyl)-phenoxymethyl polystyrene resin using 9-flourenylmethoxycarbamate (FMOC) protected amino acids as described previously (19). All of the amino acids and resins used for the solid-phase synthesis of the peptides were purchased from Bachem Bioscience Inc. (King of Prussia, PA). Acetonitrile (ACN) and trifluoroacetic acid (TFA) were purchased from Fisher Scientific (Pittsburgh, PA). All of the solvents used in these studies were of HPLC grade or better.

BBMEC Isolation and Development of Primary Cultures

BBMECs were isolated from bovine brain gray matter by enzymatic digestion using collagenase/dispase followed by Percoll gradient centrifugation as originally described by Audus and Borchardt (20) and recently modified (24). The isolated BBMECs were seeded at 50,000 cells/cm^2 onto a Transwell® filter insert (24 mm diameter), which contained a microporous polycarbonate membrane (0.4 μm pore size). The culture medium contained 25 μg/mL endothelial cell growth supplements, 45% minimum essential medium, 45% F-12 medium, 10% platelet-poor horse serum, 50 μg/mL gentamicin, and 125 μg/mL heparin. The Transwell® insert membranes were treated with rat tail collagen and fibronectin prior to seeding (20,24). The apical (AP) chamber contained 1.5 mL culture medium and the basolateral (BL) chamber contained 2.6 mL culture medium. The cells were grown in a 37°C incubator in 5% CO_2 and 95% humidity. The culture medium was changed on the third day after plating and every other day thereafter. The cultured BBMECs formed a monolayer by day 7 and a tight monolayer approximately 8 or 9 days after plating. The formation of the monolayer and its tightness were judged by staining the filamentous actin cytoskeleton of the BBMECs with rhodamine-phalloidin or by measuring the flux of [^{14}C]-sucrose across the monolayers, as described below.

Transport Studies

The transport studies were conducted using BBMEC monolayers cultured for 8 to 10 days. All of the transport studies were conducted at 37°C in pH 7.35 HBSS (modified to contain 25 mM glucose and 10 mM HEPES) buffer. All transport studies were performed in the AP to BL direction. Prior to the experiments, the cells were washed three times with HBSS. The third wash was left on the cells at 37°C for an incubation period of 10 min. Transport experiments were run for 2 hr in triplicate with receiver side sampling performed every 20 min, and donor side sampling performed every hour. When permeation rates were estimated across the collagen-coated filter support in the absence of the cells, the sampling intervals were changed to every 10 min over a 1 hr period.

The [^{14}C]-radiolabeled permeants (sucrose, urea, methylamine, lactate and formate) were applied to the donor side at approximately 0.2–0.4 nM, which gave counts of 5–7 × 10^6 dpm/mL. When aliquots (0.1 mL) were removed from the donor or receiver compartment of the BBMEC monolayers, 4 mL of scintillation cocktail was added to the sample and analysis was conducted by liquid scintillation counting. The atenolol experiments were conducted with the donor solutions containing 400 μM of permeant in HBSS. In the experiments with atenolol, receiver and donor compartment samples (0.1 mL) were diluted with HBSS (0.9 mL). The peptide transport experiments were conducted with the donor solutions containing concentrations of 300–500 μM of the permeant in HBSS. In the transport experiments with peptides, receiver samples (0.12 mL) were diluted with ACN (0.01 mL). The atenolol and the peptide samples were analyzed by gradient reversed-phase HPLC as described below.

HPLC Analysis

The atenolol and the peptide samples were analyzed by gradient reversed-phase HPLC using a Rainin Dynamax 300A C18 column (5 μm, 4.6 × 250 mm) with a Dynamax C18 guard column. The eluents for the analysis of atenolol and the Tyr-containing peptides consisted of Milli-Q H_2O:ACN:TFA in ratios of 90:10:0.1 (solvent A) and 20:80:0.1 (solvent B). The eluents for the analysis of Phe-containing peptides consisted of Milli-Q H_2O:ACN:TFA in ratios of 75:25:0.1 (solvent A) and 20:80:0.1 (solvent B). Elution of atenolol and the Tyr-containing peptides was accomplished using a gradient that consisted of ramping from 0–30% B over 12 minutes. The gradient was modified for the Phe-containing peptides to ramping from 10%–45% B over 10 min, then ramping from 45%–90% from 10–15 min. The fluorescence detector was set to excitation and emission wavelengths of 275 and 295 nm, respectively, for atenolol; 278 and 305 nm, respectively, for the Tyr-containing peptides; and 257 and 282 nm, respectively, for the Phe containing peptides. A flow rate of 1.0 mL/min was used.

Theoretical Analysis

The effective permeability coefficients (P_{eff}) were determined from the appearance kinetics of the hydrophilic permeants and the peptides in the receiver compartment at steady state (25):

$$\frac{M_R}{M_{D(0)}} = \left(\frac{V_R}{V_R + V_D}\right)\left[1 - e^{-\alpha\beta t}\right] \quad (1)$$

$$\alpha = AP_{eff}/V_D \quad (2a)$$

$$\beta = (V_R + V_D)/V_R \quad (2b)$$

where M_R is the mass in the receiver side; $M_{D(0)}$ is the initial mass in the donor side; V_R (2.6 mL) and V_D (1.5 mL) are volumes of the receiver and donor sides, respectively; t is the time; and A is the surface area of the filter support (4.71 cm^2). P_{eff} is further defined by:

$$\frac{1}{P_{eff}} = \frac{1}{P_M} + \frac{1}{P_{ABL}} + \frac{1}{P_F} + \frac{1}{P_C} \quad (3)$$

where the P_{ABL} is the permeability coefficient across the aqueous boundary layers; P_F is the permeability coefficient across the filter support; P_C is the permeability coefficient across the collagen; and P_M is the permeability coefficient of the permeant across the monolayer (23,25). P_M values are the sum of the calculated permeability coefficients for the paracellular (P_P) and transcellular (P_T) pathways (i.e., $P_M = P_P + P_T$). The contributions from P_{ABL}, P_F, and P_C can be assessed by measuring the permeability coefficients ($P_{ABL/F/C}$) of the permeants across the collagen-coated filter support. Therefore, equation 4

$$\frac{1}{P_{eff}} = \frac{1}{P_M} + \frac{1}{P_{ABL/F/C}} \quad (4)$$

can be used to obtain the permeability coefficient of the permeant across the cell monolayer only in the absence of the mass transfer resistances of the Transwell® system.

For the hydrophilic permeants, the calculated P_T can be ignored. Therefore, P_M is equivalent to the calculated P_P. The calculated P_P values for the hydrophilic permeants varying in molecular size and charge can also be obtained by (23,25):

$$P_p = \frac{\epsilon DF(r/R)}{\delta} f^{\pm}(\kappa) \quad (5)$$

where ϵ is the porosity of the monolayer; $\delta = \tau L$, the tortuosity (τ) times the path length (L) across the monolayer; D is the aqueous diffusion coefficient of the permeant; F(r/R) is the Renkin molecular sieving function; and $f^{\pm}(\kappa)$ represents dimensionless electrochemical energy functions across the electronegatively charged pore. The value of $f^{\pm}(\kappa)$ varies depending upon the charge of the permeant, where $f^{\pm}(\kappa) \geq 1$ for cationic permeants; $f^{\pm}(\kappa) = 1$ for neutral permeants; and $f^{\pm}(\kappa) \leq 1$ for anionic permeants. The dimensionless Renkin molecular sieving function (22,23,25), or hindrance function, compares the molecular radius (r) and the cylindrical pore radius (R) and takes values of $0 < F(r/R) < 1$:

Table 1. The Physicochemical Properties of the Hydrophilic Permeants Used to Determine the Aqueous Pore Radius Across the Cellular Tight Junctions of the BBMEC Monolayers

Permeant	Molecular weight	Molecular density (gm/ml)	Aqueous diffusion coefficient[a] ($\times 10^5$ cm^2/s)	Molecular radius (Å)[a]
Urea	60	1.32	1.22	2.67
Sucrose	342	1.00	0.61	5.51
Methylamine	31	0.70	1.24	2.65
Atenolol	266	1.00	0.72	4.80
Formate	46	1.22	1.30	2.51
Lactate	90	1.22	1.04	3.13

[a] Calculated from the Stokes–Einstein equation for equivalent spheres as described by Adson *et al.* (23).

$$F\left(\frac{r}{R}\right) = \left(1 - \left(\frac{r}{R}\right)\right)^2 \times \left[1 - 2.104\left(\frac{r}{R}\right) + 2.09\left(\frac{r}{R}\right)^3 - 0.95\left(\frac{r}{R}\right)^5\right] \quad (6)$$

The aqueous pore radius was calculated from the ratio of the calculated P_P values of each hydrophilic permeant pair of like charges by the following relationship, as described previously (23,25):

$$\frac{r_x P_x}{r_y P_y} = \frac{F(r_x/R)}{F(r_y/R)} \quad (7)$$

where the subscripts x and y denote the permeant pair. Since the aqueous diffusion coefficients and molecular radii (Table 1) of the hydrophilic permeants are known from the literature (23,25) and the calculated permeability coefficients of these permeants were determined in triplicate using BBMEC monolayers, the only unknown was the aqueous pore radius. Calculations of the pore radius were then performed using each combination of replicate pairs (9 combinations) to yield the average pore radius.

The values obtained for the pore radius, ϵ and δ were calculated from the sucrose and urea transport data. The value of $f^{\pm}(\kappa)$ was estimated from the lactate and formate transport data. These values were utilized along with the molecular radii of the peptides to calculate P_P^* values for the peptides. A one-way ANOVA ($r > 95\%$) with a Tukey's comparison was performed to contrast the theoretical P_P^* values with the observed P_{eff} values.

RESULTS

Determination of the Aqueous Pore Radius of the Tight Junctions in BBMEC Monolayers

The physicochemical properties of the hydrophilic permeants that were used to characterize the aqueous pore radius of the TJs in BBMEC monolayers are shown in Table 1. These permeants were selected because they are known to traverse a cellular monolayer predominantly via the paracellular route and

Table 2. Observed P_{eff} and $P_{ABL/F/C}$ Values of the Hydrophilic Permeants and the Calculated Paracellular Parameters [P_P, R, F(r/R), $f^{\pm}(\kappa)$]

Permeant	Observed P_{eff}[a] ($\times 10^6$ cm/s)		Observed $P_{ABL/F/C}$[b] ($\times 10^6$ cm/s)		Calculated P_P[c] ($\times 10^6$ cm/s)		Pore Radius[c] (R,Å)		F(r/R)[c]	$f^{\pm}(\kappa)$[c]
Urea	35.3	(3.23)	124	(7.62)	49.6	(5.28)	15.3	(1.1)	0.439	1
Sucrose	6.53	(0.63)	55.5	(7.23)	7.43	(0.67)			0.137	1
Methylamine	46.7	(9.42)	90.8	(10.3)	101	(39.5)	15.3	(5.2)	0.443	2.03
Atenolol	13.2	(0.81)	42.1	(7.20)	19.6	(2.48)			0.190	1.57
Formate	21.7	(1.86)	88.2	(4.21)	28.9	(2.70)	12.6	(2.2)	0.362	0.68
Lactate	12.2	(0.63)	71.6	(2.49)	14.7	(0.76)			0.260	0.60

Note: Permeability coefficients are expressed as the mean ± (s.d.) for n = 3.
[a] Determined using BBMEC monolayers grown onto microporous membranes as described in Materials and Methods.
[b] Determined using microporous membranes coated with collagen as described in Materials and Methods.
[c] Calculated from Equations 4–7 as described in Materials and Methods.

their physicochemical characteristics have been well characterized (23,25).

Table 2 lists the observed P_{eff} values, the observed $P_{ABL/F/C}$ values, and the calculated P_P values for the hydrophilic permeants. The effect of size and charge on the permeation rates of the permeants is illustrated in Figure 1. By comparing the calculated P_P value for each charged permeant with that of a neutral permeant of similar size (i.e., formate versus urea), the effect of the electronegatively charged pore on the transport of charged permeants becomes evident. In addition, it is obvious from the data shown in Figure 1 that the calculated P_P values for the cationic permeants are greater than those for the neutral permeants, which in turn were greater than the calculated P_P values for the anionic permeants. The trends shown here are consistent with the principles of molecular-size-restricted diffusion in an electronegative field of force (23).

Equation 7 shows that by comparing the transport of two permeants that differ in size but are of equal charge, one can calculate the aqueous pore radii through cellular TJs, as well as the Renkin molecular sieving function [F(r/R)] and the $f^{\pm}(\kappa)$. Using Equation 7, the average aqueous pore radius through the BBMEC cellular TJs (based on the data for all three pairs of hydrophilic permeants) was found to be 14.4 (±3.2) Å (Table 2). The values for the Renkin molecular sieving function [F(r/R)] clearly show the effect of size on the paracellular permeation of the hydrophilic permeants (Table 2). This is also shown graphically in Figure 2, where it is apparent that as the size of the molecule is reduced, the effect of the Renkin function on the paracellular permeability through that pore is greatly increased. The average value for ϵ/δ was found to be 8.9 cm^{-1} from the neutral permeant transport data. This value is a function of the BBMEC monolayer and is a required parameter for the calculation of the $f(\kappa)$ values for the charged permeants and the P_P^* values for the anionic model peptides.

The effect of charge on the paracellular permeation of the charged permeants is also seen in Table 2 by comparing the $f^{\pm}(\kappa)$ values for the anionic and cationic permeants. Consistent with theory (23,25), the electronegatively charged pores of cellular TJs enhance the transport of the cationic permeants while hindering the transport of the anionic permeants. There

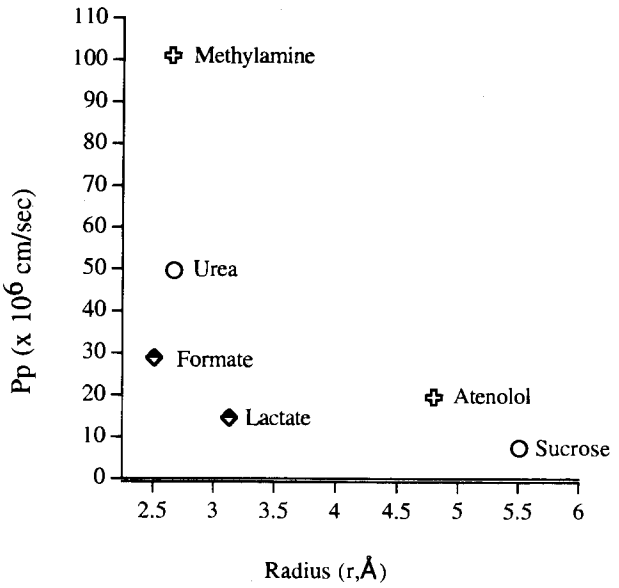

Fig. 1. A plot of the calculated P_P values for the hydrophilic permeants representing neutral, anionic, and cationic molecules versus the molecular radii (r) of the permeants.

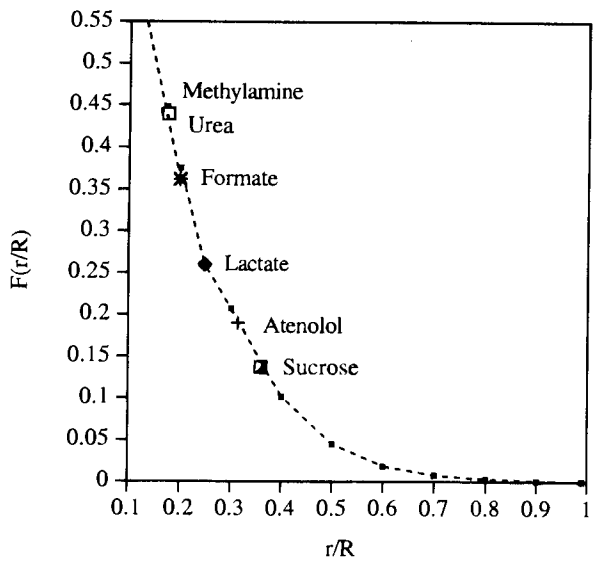

Fig. 2. A plot of the Renkin molecular sieving function [F(r/R)] versus the ratio (r/R) of the molecular radii (r) of permeants and the pore radius (R) in the TJs of the BBMEC monolayers. The dashed line represents the Renkin molecular sieving function.

is no pronounced effect of size on the f(κ) values when each pair of like charged permeants are compared.

Peptide Permeation Characteristics Across BBMEC Monolayers

The observed P_{eff} values for the model peptides are given in Table 3. With the hydrophilic Tyr-containing peptides (Ac-TyrProXaaZaaVal-NH_2; Xaa = Gly, Ile; Zaa = Asp, Asn, Ile), there was no statistically significant difference between the observed P_{eff} values of the Gly- and Ile-containing peptides within a pair. However, when the Tyr was replaced with Phe, the Gly-containing analogs (Ac-PheProGlyIleVal-NH_2 and Ac-PheProGlyIle-NH_2) were shown to have significantly higher observed P_{eff} values than the Ile-containing analogs (Ac-PheProIleIleVal-NH_2 and Ac-PheProIleIle-NH_2).

The routes (paracellular and transcellular) by which these peptides permeate the BBMEC monolayer can be approximated by comparing the observed P_{eff} values for each peptide with the P_P^* values calculated using the Renkin molecular sieving function by knowing the molecular radius (r) of each peptide and the aqueous pore radius (R) of the TJs in the BBMEC monolayers. Based on a comparison of the theoretical P_P^* values with the observed P_{eff} values shown in Table 3, it is apparent that all of the Tyr-containing peptides traverse the monolayer via the paracellular route. However, with the Phe-containing peptides, particularly the Gly-containing analogs, the larger observed P_{eff} values compared with the theoretical P_P^* values suggest a significant transcellular component to permeation.

To further characterize the pathways of permeation, a hydrophilic pair (Ac-TyrProIleAspVal-NH_2 and Ac-TyrProGlyAspVal-NH_2) and a hydrophobic pair (Ac-PheProGlyIleVal-NH_2 and Ac-PheProIleIleVal-NH_2) of peptides were selected, and a more comprehensive analysis of their permeability data was conducted. When the observed $P_{ABL/F/C}$ values are subtracted from the observed P_{eff} values for each peptide (Equation 4), one obtains the BBMEC monolayer permeability coefficients (P_M^*), which are given in Table 4. Knowing the theoretical P_P^* values and the calculated P_M^* values, one can then estimate the transcellular permeability coefficients (P_T^*) using the following relationship:

$$P_M^* = P_T^* + P_P^* \quad (8)$$

The theoretical P_T^* values determined for Ac-TyrProGlyAspVal-NH_2, Ac-TyrProIleAspVal-NH_2, and Ac-PheProIleIleVal-NH_2, when compared to the theoretical P_P^* values, suggest that these peptides traverse the BBMEC monolayers predominantly by the paracellular route. However, a comparison of the theoretical P_T^* value for Ac-PheProGlyIleVal-NH_2 with the theoretical P_P^* value suggests that this peptide traverses the monolayer predominantly by the transcellular route.

DISCUSSION

The architecture of the endothelial cells that constitute the BBB, particularly the presence of the TJs, restricts for all practical purposes the permeation of peptides to the transcellular route (8). The passive diffusion of peptides across the BBB via this route has been shown to be dependent upon molecular size, hydrophobicity, and hydrogen bonding potential (3,12–14). Recently, our laboratory has shown that these physicochemical characteristics of a peptide, as well as the ability of the molecule to permeate Caco-2 cell monolayers, a model of the intestinal mucosa, can be affected by the secondary structure of the molecule in solution (16–19).

In order to determine whether the β-turn structure of a peptide also influences its ability to permeate the BBB, we have employed in these studies a cell culture model of the BBB consisting of BBMEC monolayers grown onto microporous filter supports (20,21). In spite of efforts by various laboratories, including our own (24), to refine this *in vitro* cell culture model of the BBB by co-culturing BMECs with astrocytes (26,27) or treating the BMECs with astrocyte-conditioned media (28), these cells tend to form "leakier" monolayers *in vitro* than the

Table 3. Physicochemical Properties and the Observed and Calculated Permeability Coefficients (P_P^*, P_{eff}) of the Model Peptides

Peptides	Log $P_{o/w}$[a]	Molecular weight	Aqueous diffusion coefficient[b] ($\times 10^6$ cm^2/s)	Molecular radius[c] (Å)	Theoretical P_P^*[d] ($\times 10^6$ cm/s)		Observed P_{eff}[e] ($\times 10^6$ cm/s)	
Ac-TyrProIleAspVal-NH_2	−1.85	646	5.7	5.8	8.83	(1.0)	10.5	(0.7)
Ac-TyrProGlyAspVal-NH_2	−3.71	590	5.1	6.5	9.88	(1.1)	12.2	(0.9)
Ac-TyrProIleAsnVal-NH_2	−0.417	645	6.5	4.7	11.4	(1.4)	9.39	(2.2)
Ac-TyrProGlyAsnVal-NH_2	−2.06	589	7.5	4.4	15.1	(1.6)	7.77	(1.0)
Ac-TyrProIleIleVal-NH_2	1.13	644	5.7	5.7	6.43	(1.0)	9.12	(0.9)
Ac-TyrProGlyIleVal-NH_2	−0.20	588	7.2	4.8	12.2	(1.5)	6.68	(1.1)
Ac-PheProIleIleVal-NH_2	1.61	628	6.2	5.4	8.73	(1.5)	9.35	(2.8)
Ac-PheProGlyIleVal-NH_2	1.96	572	6.4	5.1	9.57	(1.6)	42.2[f]	(1.7)
Ac-PheProIleIle-NH_2	1.17	529	6.1	5.4	8.18	(0.9)	16.7[f]	(4.8)
Ac-PheProGlyIle-NH_2	2.00	473	7.3	4.5	14.4	(1.6)	58.6[f]	(4.3)

Note: Permeability coefficients are expressed as the mean ± (s.d.) for n = 3.
[a] The log of the partition coefficients of the peptides were determined in 1-octanol:HBSS (19).
[b] Aqueous diffusion coefficients were obtained in HBSS by stop-flow capillary electrophoresis (18).
[c] The molecular radii (r) were calculated by the Stokes-Einstein equation (23).
[d] Calculated using the Renkin molecular sieving function as described in Materials and Methods.
[e] Determined using BBMEC monolayers grown onto microporous membranes as described in Materials and Methods.
[f] Denotes that the theoretical P_P^* is statistically different from observed P_{eff}.

Table 4. Transcellular and Paracellular Permeability Coefficients Derived from the Effective Permeability Coefficients for the Model Peptides

Peptide	Observed P_{eff}[a] ($\times 10^6$ cm/s)		Observed $P_{ABL/F/C}$[b] ($\times 10^6$ cm/s)		Calculated P_M^*[c] ($\times 10^6$ cm/s)		Theoretical P_P^*[d] ($\times 10^6$ cm/s)		Theoretical P_T^*[e] ($\times 10^6$ cm/s)	% Transcellular
Ac-TyrProIleAspVal-NH_2	10.5	(0.8)	76.7	(7.0)	12.2	(0.8)	8.83	(1.0)	3.4	28
Ac-TyrProGlyAspVal-NH_2	12.2	(0.9)	102	(9.1)	13.9	(0.9)	9.88	(1.1)	4.0	29
Ac-PheProIleIleVal-NH_2	9.35	(2.8)	83.7	(21)	10.7	(3.0)	8.73	(1.5)	2.0	18
Ac-PheProGlyIleVal-NH_2	42.2	(1.7)	63.0	(8.0)	139[f]	(38)	9.57	(1.5)	129.4	93

Note: Permeability coefficients are expressed as the mean ± (s.d.) for n = 3.
[a] Determined using BBMEC monolayers grown onto microporous membranes as described in Materials and Methods.
[b] Determined using microporous membranes coated with collagen as described in Materials and Methods.
[c] Calculated from Equation 4 as described in Materials and Methods.
[d] Calculated using the Renkin molecular sieving function (Equation 6) and the paracellular permeability equation (Equation 5) as described in Materials and Methods.
[e] Calculated from $P_M = P_P + P_T$ as described in Materials and Methods.
[f] Denotes that the theoretical P_P^* is statistically different from calculated P_M^*.

in vivo BBB (8). Therefore, to circumvent this "leakiness" problem, we decided to exploit a mathematical approach using the Renkin molecular sieving function to delineate the paracellular and transcellular permeability coefficients of a peptide. Recently, this approach was used successfully to elucidate the rate-determining steps and the factors that affect the paracellular diffusion of molecules and to delineate the paracellular permeation of various solutes across Caco-2 cell monolayers (23,25).

Crucial to the successful application of this mathematical approach to estimating the paracellular and transcellular permeability coefficients of a peptide across BBMEC monolayers was the determination of the aqueous pore radius of the TJs in this cell culture model. Using a series of well-characterized hydrophilic solutes (Table 2), the aqueous pore radius through the BBMEC TJs was estimated to be 14.4 ± 3.2 Å (range 12.6–15.3 Å). This value is significantly different than the cylindrical pore radius of 125 Å reported previously by van Bree *et al.* (22) for a similar cell culture system. It should be noted, however, that the cell culture conditions and the experimental conditions used in our transport studies were quite different from those used by van Bree *et al.* (22), and could account for the very different pore radius observed. Our pore radius value (14.4 ± 3.2 Å) for the BBMEC monolayers is similar, but significantly larger, than that reported by Fenstermacher and Johnson (8) for the *in vivo* BBB (7–9 Å). The larger pore radius observed in BBMEC monolayers is consistent, however, with the reported "leakiness" of this *in vitro* model as compared to the *in vivo* BBB.

Knowing the aqueous pore radius of our BBMEC culture model and the molecular radii of the model peptides used in our studies, it was possible to calculate, using the Renkin molecular sieving function, a theoretical P_P^* value for each model peptide through the cell monolayer. In addition, having the theoretical P_P^* value and a calculated P_M^* value (obtained from the experimentally determined P_{eff} and $P_{ABL/F/C}$ values), it was possible to factor out a theoretical P_T^* value for each molecule. Thus, in spite of the apparent "leakiness" of the cell culture model, one can mathematically factor out the important parameter P_T^* for a series of peptides and, thus, establish a meaningful structure-transport relationship for the major (transcellular) pathway across the BBB. It should be noted that this mathematical approach, if applied to the various cell culture models of the BBB that have been developed (e.g., 26–28), can be used to generate P_T^* values of peptides that are comparable across models irrespective of their "leakiness."

In order to investigate the relationship between the solution conformation of model peptides and their transcellular and paracellular permeability coefficients across BBMEC monolayers, we used a series of model peptides that have been shown to form varying degrees of β-turn structures in solution (Ac-TyrProXaaZaaVal-NH_2, Ac-PheProXaaIleVal-NH_2, and Ac-PheProXaaIle-NH_2; Xaa = Gly, Ile and Zaa = Asp, Asn, Ile) (19). In this series of peptides, the Gly-containing peptides were shown to exhibit significantly higher amounts of β-turn structure than their corresponding Ile-containing analogs (19). These peptides were also designed to cover a range of lipophilicities (log $P_{o/w} \approx -4.0$ to 2.0), as determined by log $P_{o/w}$ (Table 3), from hydrophilic (Ac-TyrProXaaZaaVal-NH_2; Xaa = Gly, Ile and Zaa = Asp, Asn, Ile) to hydrophobic (Ac-PheProXaaIle-Val-NH_2 and Ac-PheProXaaIle-NH_2; Xaa = Gly, Ile), enabling them to traverse BBMEC monolayers predominantly by either the paracellular (hydrophilic peptides) route or the transcellular (hydrophobic peptides) route (19). It is interesting to note that for the hydrophilic peptides, the log $P_{o/w}$ values of the Gly-containing peptides are lower than those for the Ile-containing analogs (e.g., Ac-TyrProIleAspVal-NH_2, log $P_{o/w} = -1.85$; Ac-TyrProGlyAspVal-NH_2, log $P_{o/w} = -3.71$). This observation is consistent with the more hydrophobic nature of the side chain of Ile compared to that of Gly (29). However, this trend was reversed in the hydrophobic peptides, where the log $P_{o/w}$ values of the Gly-containing peptides were higher than those for the Ile-containing analogs (e.g., Ac-PheProGlyIleVal-NH_2, log $P_{o/w} = 2.00$; Ac-PheProIleIleVal-NH_2, log $P_{o/w} = 1.17$). These results suggest that in hydrophobic peptides the influence of secondary structure (e.g., β-turns in Gly-containing peptides) on the overall hydrophobicity (as measured by log $P_{o/w}$) must be more significant than the substitution of Ile for Gly in the primary sequence of these peptides.

By comparing the theoretical P_P^* values for each peptide with its experimentally observed P_{eff} values, one can qualitatively estimate the pathway by which the peptide permeates the BBMEC monolayer. By comparison of the theoretical P_P^* values and the observed P_{eff} values obtained for the three pairs of hydrophilic peptides (Ac-TyrProXaaZaaVal-NH_2; Xaa =

Gly, Ile and Zaa = Asp, Asn, Ile), it was apparent that these peptides traverse the BBMEC monolayers predominantly via the paracellular route (i.e., the P_{eff} value is approximately equal to the theoretical P_P^* value for each peptide). It must be emphasized that this is quite qualitative, since the P_{eff} values have not been corrected for mass transfer resistances of the Transwell® system (the observed $P_{ABL/F/C}$). It is also apparent from the data shown in Table 3 that the hydrophilic peptides having more β-turn structure (i.e., the Gly-containing peptides) permeate the BBMEC monolayer at a rate equal to those peptides that do not exhibit this type of secondary structure (i.e., the Ile-containing peptides). Thus, the presence of β-turn structure in a hydrophilic peptide does not enhance its paracellular permeation of this cell monolayer. It is also interesting to compare the Asp-containing peptides, which have a negative charge, with the other hydrophilic peptides that have Asp replaced with a neutral Asn or Ile residue. The permeability coefficients of all of these peptides are approximately equivalent, and equal to the theoretical P_P^* values. Thus, there was no effect of charge on the paracellular permeation of these hydrophilic peptides. The same results were observed in unperturbed Caco-2 cell monolayers with this series of peptides (19) and with a series of hexapeptides (15). The Caco-2 cell monolayer has an average aqueous pore radius of approximately 5 Å, suggesting that with penta- and hexapeptides, size is the predominant factor in determining the permeation via the paracellular route.

However, it is interesting to note that when the TJs of the Caco-2 cell monolayers were perturbed with palmitoyl-DL-carnitine (PC), resulting in modulation of the aqueous pore radius, Ac-TyrProGlyAsnVal-NH_2 was found to have a significantly higher permeation rate than that of Ac-TyrProIleAsnVal-NH_2 (19). These results are obviously different than the results observed for this pair of peptides in the BBMEC monolayers. This was particularly surprising to us because when the Caco-2 cell monolayer is perturbed with PC, its TJs have an average aqueous pore radius of approximately 12 Å, which is very similar to the value of approximately 14 Å observed in this study for the BBMEC monolayers. One possible explanation for this difference may be the architecture of these cell monolayers; Caco-2 cells are columnar epithelial cells, which tend to grow taller [average cell height of ≈20 μm (30)] than the BBMEC cells [average cell height of ≈0.5 μm (26)]. Thus, Caco-2 cell monolayers have longer tortuous lateral space than BBMEC monolayers. The lateral space of the perturbed Caco-2 cell monolayers was estimated to be approximately 20% of the barrier to paracellular diffusion (25). The contribution of the lateral space to paracellular diffusion across BBMEC monolayers would not be expected to be as large. Other possible explanations for these differences would include: (a) different cell densities (i.e., Caco-2 cell densities are much higher then the BBMEC cell densities at confluency which may also effect the lateral space); and (b) differences in the distribution of gap junctions and/or desmosomes between the cell culture models, which would also influence the lateral space distribution.

When comparisons were made between the theoretical P_P^* values and the observed P_{eff} values obtained for the hydrophobic peptides, it was apparent that the most hydrophobic pair of peptides (Ac-PheProIleIle-NH_2 vs. Ac-PheProGlyIle-NH_2) permeate BBMEC monolayers predominantly via the transcellular pathway. In addition, in this pair, the Gly-containing peptide, which has the highest degree of β-turn structure, was able to permeate BBMEC monolayers most readily. It is interesting to note that this Gly-containing peptide was more lipophilic as estimated by log $P_{o/w}$ than the Ile-containing peptide. In the other pair of hydrophobic peptides (Ac-PheProIleIleVal-NH_2 vs. Ac-PheProGlyIleVal-NH_2), the Gly-containing peptide appears to permeate BBMEC monolayers predominantly via the transcellular pathway, whereas the Ile-containing peptide appears to permeate this cell monolayer predominantly via the paracellular route.

Further insights into the route of permeation that a peptide favors can be made using the theoretical P_P^* value of a peptide and Equation 8. The theoretical P_T^* value for that peptide can then be calculated using the experimentally determined P_M value. The P_M value can be calculated from the experimentally determined P_{eff} and $P_{ABL/F/C}$ values by Equation 3. This approach was then applied to the data (Table 4) for the most hydrophilic (Ac-TyrProIleAspVal-NH_2 vs. Ac-TyrProGlyAspVal-NH_2) and hydrophobic (Ac-PheProIleIleVal-NH_2 vs. Ac-PheProGlyIleVal-NH_2) pentapeptide pairs. The results of these studies confirm that the permeation of the hydrophilic peptides occurs predominantly via the paracellular route (≈72% paracellular permeation). Ac-PheProIleIleVal-NH_2 transport across the BBMEC monolayer was also found to occur predominantly via the paracellular route (≈80% paracellular permeation). However, Ac-PheProGlyIleVal-NH_2 was shown to traverse the BBMEC monolayer almost exclusively via the transcellular route (≈95% transcellular permeation). This confirms that the ability of hydrophobic peptides to form β-turns in solution can significantly influence their ability to permeate BBMEC monolayers via the transcellular route.

In conclusion, we have shown in this study that the aqueous pore radius through the BBMEC TJs can be determined by using the Renkin molecular sieving function. This value can then be used to estimate the theoretical P_P^* value of a peptide, enabling us to determine the extent to which a peptide crosses BBMEC monolayers via both the paracellular and transcellular routes. This approach can be applied as a correction for transport data obtained in different cell culture models where variability exists in the pores of the TJs. In addition, the results of these studies suggest that a hydrophobic peptide that exhibits significant β-turn structure will be more lipophilic as measured by log $P_{o/w}$ and will more readily permeate a cellular monolayer via the transcellular route than a hydrophobic peptide that lacks this type of solution structure. In contrast, similar secondary structural features in hydrophilic peptides do not appear to alter the physicochemical characteristics of the molecule sufficiently to increase the paracellular flux through the aqueous pores.

ACKNOWLEDGMENTS

This work was supported in part by the United States Public Health Service (GM-51633 and GM-088359) and the Costar Corporation. We would also like to thank Dr. Kenneth L. Audus and Mrs. Jayna Rose for their advice and cooperation.

REFERENCES

1. W. M. Pardridge (ed.). *Peptide Drug Delivery to the Brain*, Raven Press, New York; 1991.
2. K. L. Audus, P. J. Chikhale, D. W. Miller, S. E. Thompson, and R. T. Borchardt. in B. Testa (ed.), *Advances in Drug Research: Volume 23*, Harcourt Brace Jovanovich, London; 1992, pp. 1–64.

3. D. J. Begley. *J. Controlled Release* **29**:293–306 (1994).
4. M. W. Brightman. *Exp. Eye Res.* **25**:1–25 (1977).
5. B. Schlosshauer. *BioEssays* **15**:341–346 (1993).
6. W. M. Pardridge (ed.). *The Blood-Brain Barrier: Cellular and Molecular Biology*, Raven Press, New York; 1993.
7. G. W. Goldstein and A. L. Betz. *Scientific American* **255**:70–79 (1986).
8. J. D. Fenstermacher and J. A. Johnson. *Am. J. Physiol.* **211**:341–346 (1966).
9. W. M. Pardridge. *Physiol. Rev.* **63**:1481–1535 (1983).
10. E. G. Chikhale, P. S. Burton, and R. T. Borchardt. *J. Pharmacol. Exp. Ther.* **273**:298–303 (1995).
11. W. M. Pardridge. in M. D. Taylor and G. L. Amidon (eds.), *Peptide-Based Drug Design*, American Chemical Society, Washington, D.C.; 1995, pp. 265–296.
12. W. M. Pardridge. *Adv. Drug Del. Rev.* **15**:3–36 (1995).
13. W. A. Banks and A. J. Kastin. *Brain Res. Bull.* **15**:287–292 (1985).
14. E. G. Chikhale, K. Y. Ng, P. S. Burton, and R. T. Borchardt. *Pharm. Res.* **11**:412–419 (1994).
15. G. M. Pauletti, F. W. Okumu, and R. T. Borchardt. *Pharm. Res.* **14**:164–168 (1997).
16. F. W. Okumu, G. M. Pauletti, D. G. Vander Velde, T. J. Siahaan, and R. T. Borchardt. *Pharm. Res.* **14**:169–175 (1997).
17. S. Gangwar, S. D. S. Jois, T. J. Siahaan, D. G. Vander Velde, V. J. Stella, and R. T. Borchardt. *Pharm. Res.* **13**:1657–1662 (1996).
18. G. M. Pauletti, S. Gangwar, F. W. Okumu, T. J. Siahaan, V. J. Stella, and R. T. Borchardt. *Pharm. Res.* **13**:1615–1623 (1996).
19. G. T. Knipp, D. G. Vander Velde, T. J. Siahaan, and R. T. Borchardt. *Pharm. Res.* **14**:1332–1340 (1997).
20. K. L. Audus and R. T. Borchardt. *Pharm. Res.* **3**:81–87 (1986).
21. K. L. Audus and R. T. Borchardt. *Ann N. Y. Acad. Sci.* **507**:9–18 (1987).
22. J. B. M. M. van Bree, A. G. de Boer, M. Danhof, L. A. Ginsel, and D. D. Breimer, *J. Pharmacol. Exp. Ther.* **247**:1233–1239 (1988).
23. A. Adson, T. J. Raub, P. S. Burton, C. L. Barsuhn, A. R. Hilgers, K. L. Audus, and N. F. H. Ho. *J. Pharm. Sci.* **83**:1529–1536 (1994).
24. K. L. Audus, L. Ng, W. Wang, and R. T. Borchardt. in P. L. Smith, R. T. Borchardt, and G. Wilson (eds.), *Models for Assessing Drug Absorption and Metabolism*, Plenum Press, New York; 1996, pp. 239–258.
25. G. T. Knipp, N. F. H. Ho, C. L. Barsuhn, and R. T. Borchardt. *J. Pharm. Sci.* **86** (1997). In press.
26. T. J. Raub, S. L. Kuentzel, and G. A. Sawada. *Exp. Cell Res.* **199**:330–340 (1992).
27. J.-H. Tao-Cheng, Z. Nagy, and M. W. Brightman. *J. Neuroscience* **7**:3293–3299 (1987).
28. J. Laterra, C. Guerin, and G. W. Goldstein. *J. Cell. Physiol.* **144**:204–215 (1990).
29. D. Eisenberg, M. Wesson, and W. Wilcox. in G. Fasman (ed.), *Prediction of Protein Structure and the Principles of Protein Conformation*, Plenum Press, New York; 1989, pp. 635–646.
30. G. Wilson, I. F. Hassan, C. J. Dix, I. Williamson, R. Shah, M. Mackay, and P. Artursson. *J. Controlled Release* **11**:25–40 (1990).